ANISOTROPIC IMAGE SHARPENING VIA WELL-POSED SOBOLEV GRADIENT FLOWS

J. CALDER AND A. MANSOURI

Abstract. We study well-posed perturbations of formally ill-posed diffusion equations which are used in image processing, such as the Perona–Malik equation. Our perturbation technique is to consider the diffusion equations as L^2 gradient flows on integral functionals and then modify the inner product from L^2 to a Sobolev inner product. We show that the functional differential equations obtained in this way are well-posed in both the forward and backward directions. We then show how to design a well-posed image sharpening algorithm via Sobolev gradient ascent on a Perona–Malik type functional. We provide full numerical implementation details and show experimental results on natural images which suggest that this method outperforms previous work by the authors as well as other sharpening algorithms such as the shock filter.

Key words. Image Sharpening, Image Diffusion, Perona–Malik Paradox, Partial Differential Equations, Gradient Descent, Gradient Ascent, Sobolev Spaces

1. Introduction. Partial differential equation (PDE) methods in image processing have proven to be fundamental tools for image diffusion and enhancement [41, 38, 42, 13, 2, 1, 3, 49, 47, 48, 52, 4]. Many diffusion PDE, such as the Perona–Malik and You–Kaveh models [41, 52], can be interpreted as the L^2 gradient descent equations on an integral functional

$$E[u] = \int_\Omega \phi(|\nabla u|^2, |\Delta u|^2)\ dx, \tag{1.1}$$

where $\Omega \subset \mathbb{R}^n$ is the image domain and $u : \Omega \to \mathbb{R}$ is a grayscale image function. For the task of image diffusion, one wishes to preserve edges while smoothing fine details and noise. For such a task, concave potentials ϕ with sublinear growth have proven effective. For example, one variant of the Perona–Malik equation can be obtained by taking $\phi(x, y) = \ln(1 + x/K^2)$, while a similar variant of the You–Kaveh equation corresponds to $\phi(x, y) = \ln(1 + y/K^2)$ where $K > 0$ is a constant.

The choice of concave potentials for the Perona–Malik model yields a class of forward-backward diffusion equations which typically do not admit classical or distributional solutions [17, 27, 51]. This poses a serious challenge to any well-posedness theory for these important image processing PDE; indeed there are numerous non-existence results for the Perona–Malik PDE [30, 54, 25]. Despite its formal ill-posedness, the Perona–Malik PDE admits discretizations which yield stable numerical results. This seemingly paradoxical result has been termed the Perona–Malik Paradox [30].

Although there is much literature on image diffusion, there are relatively few image enhancement PDE in the literature. This may be attributed to the fact that the exact features one would like from a sharpening PDE also tend to cause ill-posedness. Perhaps the most well-known sharpening PDE is the shock filter [38, 39] which is a non-linear variant on the reverse heat equation. Aside from the shock filter, other combined sharpening and smoothing PDE have been proposed based on a Perona–Malik scheme where ϕ is allowed to have a negative derivative [24] which leads to sharpening of certain gradients. Although these models encounter the same ill-posedness problems as the Perona–Malik equation, sophisticated discretizations have been proven stable [50].

We consider in this paper a perturbation of the Perona–Malik style diffusion equations which yields a class of well-posed image diffusion and sharpening equations.

Building upon our previous work [10, 11], we study the gradient descent equations on high-order generalizations of (1.1) with respect to various Sobolev inner products. We establish a very general existence and uniqueness result which applies to a family of high order diffusion/sharpening equations which are generalizations of the Perona–Malik and You–Kaveh equations. Our method of perturbing the Perona–Malik equation is different than previous works [13] in the fact that the resulting PDE is still a gradient descent PDE on the exact same functional. We then show how to choose the potential function ϕ to design a sharpening algorithm which sharpens strong image features while suppressing noise. We also provide details on our numerical methods and show experimental results.

2. Background.

2.1. Anisotropic diffusion PDE. The Perona–Malik equation (and its variants)

$$u(0) = u_0, \quad \frac{du}{dt} = \operatorname{div}(g(|\nabla u|^2)\nabla u), \quad t > 0, \tag{2.1}$$

on the domain $\Omega \subset \mathbb{R}^n$ with Neumann boundary conditions are perhaps some of the most widely used PDE in image processing [41, 42, 13, 2, 1, 49, 47, 48]. Note that u_0 is the image to be processed. Perona and Malik proposed two diffusion coefficients

$$g(s^2) = \frac{1}{1 + s^2/K^2}, \quad \text{and} \quad g(s^2) = e^{-s^2/K^2},$$

where $K > 0$ is a constant. The first equation stems from the concave potential $\phi(s^2) = \ln(1 + s^2/K^2)$ and results in a formally ill-posed diffusion equation. It was shown by Kichenassamy [30] that any weak solution to the Perona–Malik equation in one dimension must posses an infinitely differentiable initial condition wherever its gradient exceeds K. Even if u_0 is smooth, this result shows that there are minor perturbations of the initial value problem for which weak solutions do not exist, and hence the Perona–Malik PDE is ill-posed in the sense of Hadamard.

On the other hand, it is well-known that the Perona–Malik PDE admits simple and stable discretizations. This discrepancy between numerical and theoretical results has received a lot of attention within the mathematics and imaging communities [46, 25, 22, 23, 54, 6, 7, 20, 18, 15, 35]. Zhang et al. [54] established that the one-dimensional Perona–Malik equation admits infinitely many weak solutions. Gobbino et al. [25] showed that every C^1 solution to the one-dimensional Perona–Malik equation on $\mathbb{R}$ is an affine function of the form $u(x,t) = ax + b$. Ghisi et al. [23] established the existence of local-in-time classical solutions for the one-dimensional Perona–Malik equation with initial condition belonging to a class of functions which are dense in $C^1([-1,1])$. Taheri et al. [46] and Chen et al. [15] showed that there exist infinitely many Young measure solutions [12] to both the one and two-dimensional Perona–Malik equations. Bellettini et al. [6, 7] examined a perturbed Perona–Malik functional and showed that the Γ-limit [16, 8] is a free-discontinuity functional which may help to explain the staircaising phenomenon. Morini et al. [35] established that a family of discrete Perona–Malik energies Γ-converges to an anisotropic Mumford–Shah functional [36]. Esedoḡlu [18, 19] analyzed the discretization of the one dimensional Perona–Malik scheme and showed that by scaling the parameter K in proportion to the discretization step size, one can obtain a meaningful continuum limit as a system of heat equations coupled through their boundary conditions.

Other work has been focused on how to modify or regularize the Perona–Malik PDE to obtain a related well-posed model. For example, Catté, Lions, Morel, and Coll [13] proposed to replace $g(|\nabla u|^2)$ by $g(|\nabla(G_\sigma * u)|^2)$ in the Perona–Malik equation. Since differentiation is highly susceptible to noise, such a technique is commonly used in the image processing community to robustly estimate discrete derivatives [33]. They prove existence, uniqueness and regularity for the related model and demonstrate experimentally that the related model gives similar results to the Perona–Malik equation.

One drawback of the Perona–Malik model is the staircasing effect in which discontinuities (staircasing) are introduced into an image in areas of weak gradient. In an effort to mitigate these staircasing artifacts, You and Kaveh [52] have proposed a fourth order generalization of the Perona–Malik equation

$$u(0) = u_0, \quad \frac{du}{dt} = \Delta(g(|\Delta u|^2)\Delta u), \quad t > 0. \tag{2.2}$$

This model does indeed mitigate the staircasing phenomenon (gradient singularities), but at the cost of introducing singularities in the Laplacian which appear as speckle artifacts in the processed image. See Greer et al. [26] for a study singularities in the You-Kaveh equation. You and Kaveh use the same diffusion coefficient as in the Perona–Malik equation and hence (2.2) is also ill-posed.

2.2. Image enhancement PDE. Osher and Rudin [38] proposed the shock filter for image enhancement and deconvolution

$$u(0) = u_0, \quad \frac{du}{dt} = -|\nabla u|\mathcal{L}(u), \quad t > 0, \tag{2.3}$$

where $\mathcal{L}$ is an edge detecting operator. Typical choices for $\mathcal{L}$ are

$$\mathcal{L}(u) = \frac{\Delta u}{1 + |\Delta u|}, \quad \text{and} \quad \mathcal{L}(u) = \frac{u_{\eta\eta}}{1 + |u_{\eta\eta}|},$$

where $u_{\eta\eta} = \sum_{i,j} u_{x_i} u_{x_j} u_{x_i x_j}$ is the second derivative in the direction of the gradient ∇u. From a mathematical point of view, this PDE looks severely ill-posed. However, Rudin and Osher [38] devised a sophisticated numerical scheme which gives very satisfying results. There are at present no known theoretical results in the literature concerning the existence or uniqueness of solutions to this PDE. Rudin and Osher [38] have conjectured that for continuous initial data $u_0(x)$, the one dimensional shock filter has a unique solution which is continuous everywhere except at a finite number of points which correspond to the inflection points of u_0. The shock filter can be combined with anisotropic diffusion in a well-posed sharpening and smoothing framework [3].

Gilboa, Sochen and Zevvi [24] proposed a forwards and backwards diffusion model based on the Perona–Malik model (2.1) with diffusion coefficient

$$g(s) = \frac{1}{1 + (s/k_f)^n} - \frac{\alpha}{1 + ((s - k_b)/w)^{2m}}, \tag{2.4}$$

where k_f, k_b, w, m, n are all constants. Such a model behaves like the smoothing Perona–Malik model for weak gradients but becomes a reverse diffusion process for large gradients. They give a stability condition in the one-dimensional case, but the two-dimensional model has observed instabilities [50]. A sophisticated numerical method has been proposed for these types of PDE and is provably stable [50]. However, these stability results are discrete and rely heavily on the relative amounts of smoothing and sharpening.

2.3. Previous and related work. Sobolev gradients have been recently studied in the context of active contours [44, 43, 45] and image decomposition [29]. In [44, 43, 45], the gradient descent PDE for segmentation and tracking energies are recast under a Sobolev metric. The resulting tracking and segmentation algorithms, referred to as Sobolev active contours, are found to be far more robust with respect to noise and more global in nature. In a similar fashion, Charpiat et al. [14] study the case for active contours in more generality and show how to design inner products in order to achieve a desired amount of spatial coherency in the gradient flow. Richardson [29] studied the use of Sobolev gradients for image decomposition tasks [32, 5, 34], which involve the minimization of a least squares functional. By considering the gradient flow for these minimizations with respect to a Sobolev metric, one can avoid falling into irrelevant local minima and obtain faster convergence rates. Richardson [28] also studied the use of high order Sobolev gradients for the purpose of solving nonlinear differential equations via a gradient descent algorithm on a least squares functional.

The common trend in the previous works on Sobolev gradients is the recasting of a gradient descent algorithm under a Sobolev inner product in order to achieve better convergence results and less susceptibility to local minima. Oftentimes, the desired critical points are solutions to some PDE and Sobolev gradient descent is used merely as a tool for finding these solutions. Sobolev gradients and differential equations have been studied extensively in this context; a good reference is Neuberger's book [37]. What matters in these approaches is *only* that the gradient descent PDE converges to a critical point of the associated energy functional. As such, much of the theory on Sobolev gradients and differential equations is focused on studying when the gradient flows converge as $t \to \infty$ [37].

We study Sobolev gradients because they yield well-posed image sharpening flows. As such, our main concern is the existence and uniqueness of solutions to these gradient flow PDE and *not* the convergence (or lack-thereof) as $t \to \infty$ to minima or maxima. In this framework, the desired image is not an energy minimizer, it is simply one image out of a family of progressively sharper images. The task of picking the desired image out of this family is equivalent to selecting a stopping time for the gradient flow, which can be done by selecting a desired sharpness factor. The PDE will then be run until the initial image has been sharpened by the desired factor, as measured by an appropriate image sharpness measure. We discuss this further in section 6.

This work is an extension of previous work by the authors [10, 11] which focused on the isotropic equations

$$u(0) = u_0, \quad \frac{du}{dt} = \pm(I - \lambda\Delta)^{-k}\Delta u, \quad t > 0,$$

which can be interpreted as gradient flows on the heat equation energy with respect to H^k inner products. The reverse flow was shown to be an effective linear sharpening algorithm and, when combined with higher order standard diffusions, yields interesting smoothing/sharpening effects. In this work, we extend the results of [10, 11] to nonlinear anisotropic diffusion equations of arbitrary order. The anisotropic nature of these gradient ascent flows allows us to construct image sharpening algorithms which sharpen only the coarse structures in the image while suppressing noise and fine details.

We should note that Sobolev regularization of ill-posed parabolic PDE has been studied previously as a model for aggregating populations [40]. The model is given

by:

$$\begin{cases} u_t = \Delta(f(u) + \lambda u_t), & x \in \Omega, t > 0 \\ \eta \cdot \nabla(f(u) + \lambda u_t) = 0, & x \in \partial\Omega, t > 0 \\ u(x,0) = u_0(x), \end{cases} \tag{2.5}$$

where η is the outward unit normal to $\partial\Omega$. This model is closely related our proposed Sobolev Perona–Malik PDE, however, there are two key differences. If we develop the right hand side of (2.5), we get $\Delta f(u) = \operatorname{div}(f'(u)\nabla u)$. Hence, this model is a Perona–Malik type PDE where the diffusion coefficient depends only on u (and not on ∇u). Also, only a first order Sobolev regularization is considered in [40]. In our model, we consider Sobolev regularization of anisotropic diffusion PDE of arbitrary order.

3. Our proposed model. From here on, we will assume that the domain of our images $\Omega \subset \mathbb{R}^n$ is open and has a smooth boundary $\partial\Omega$.

3.1. Sobolev gradients. Consider a functional $E : H_0^k(\Omega) \to \mathbb{R}$ on the Sobolev space $H_0^k(\Omega)$ and suppose E is Gâteaux differentiable at $u \in H_0^k(\Omega)$, i.e. there exists a bounded linear functional $dE(u) : H_0^k(\Omega) \to \mathbb{R}$ such that

$$dE(u)v = \left.\frac{d}{dt}\right|_{t=0} E(u + tv),$$

for all $v \in H_0^k(\Omega)$. Let $\mathcal{G} : H_0^k(\Omega) \times H_0^k(\Omega) \to \mathbb{R}$ be an inner product on $H_0^k(\Omega)$. Then the gradient $\nabla_{\mathcal{G}} E(u)$ of E at u, if it exists, is the unique element of $H_0^k(\Omega)$ satisfying

$$dE(u)v = \mathcal{G}(\nabla_{\mathcal{G}} E(u), v), \tag{3.1}$$

for all $v \in H_0^k(\Omega)$. We will call $\mathcal{G}$ a *compatible* inner product if it induces a norm which is equivalent to the standard norm on $H_0^k(\Omega)$. It is immediate that if $\mathcal{G}$ is compatible, then the existence of $\nabla_{\mathcal{G}} E(u)$ follows from the Riesz representation theorem wherever E is Gâteaux differentiable. We define the gradient descent equation on E with respect to $\mathcal{G}$ to be the functional differential equation

$$u(0) = u_0, \quad \frac{du}{dt}(t) = -\nabla_{\mathcal{G}} E(u(t)), \quad t > 0. \tag{3.2}$$

We obtain the gradient ascent equation simply by removing the minus sign in (3.2). As an example, consider the Perona–Malik functional $PM_\phi(u) = \frac{1}{2}\int_\Omega \phi(|\nabla u|^2)dx$. Integration by parts yields

$$dPM_\phi(u)v = \int_\Omega \phi'(|\nabla u|^2)\nabla u \cdot \nabla v dx = \langle -\operatorname{div}(\phi'(|\nabla u|^2)\nabla u), v\rangle_{L^2(\Omega)},$$

where $u \in H^2(\Omega) \cap H_0^1(\Omega)$ and $v \in H_0^1(\Omega)$. Hence the gradient descent equation on PM_ϕ with respect to the L^2 inner product is exactly the Perona–Malik equation with diffusion coefficient ϕ'.

Let $\mathcal{G}$ be a compatible inner product on $H_0^k(\Omega)$. It follows from the Riesz Representation theorem that there exists a linear operator $\mathcal{L}_{\mathcal{G}} : H^{-k}(\Omega) \to H_0^k(\Omega)$ such that

$$\mathcal{G}(\mathcal{L}_{\mathcal{G}} u, v) = \langle u, v\rangle_{H^{-k}, H_0^k}, \tag{3.3}$$

for all $u \in H^{-k}(\Omega)$ and $v \in H_0^k(\Omega)$. Here, $\langle u, v\rangle_{H^{-k},H_0^k}$ denotes the action of the distribution $u \in H^{-k}(\Omega)$ on $v \in H_0^k(\Omega)$. It follows immediately that $\mathcal{L}_\mathcal{G}$ is bounded as well. Indeed, we have

$$\|\mathcal{L}_\mathcal{G} u\|^2_{H_0^k(\Omega)} \leq C\mathcal{G}(\mathcal{L}_\mathcal{G} u, \mathcal{L}_\mathcal{G} u) = C|\langle u, \mathcal{L}_\mathcal{G} u\rangle_{H^{-k},H_0^k}| \leq C\|u\|_{H^{-k}(\Omega)}\|\mathcal{L}_\mathcal{G} u\|_{H_0^k(\Omega)},$$

for all $u \in H^{-k}(\Omega)$. Consider now the situation where the L^2 gradient $\nabla_{L^2} E(u)$ of some functional $E : H_0^k(\Omega) \to \mathbb{R}$ is known and we wish to find the gradient $\nabla_\mathcal{G} E(u)$. Hence, we wish to find the element of $H_0^k(\Omega)$ which satisfies

$$\mathcal{G}(\nabla_\mathcal{G} E(u), v) = dE(u)v = \langle \nabla_{L^2} E(u), v\rangle_{L^2} = \langle \nabla_{L^2} E(u), v\rangle_{H^{-k},H_0^k},$$

for all $v \in H_0^k(\Omega)$. But this is exactly the defining quality of $\mathcal{L}_\mathcal{G}$, thus we obtain that

$$\nabla_\mathcal{G} E(u) = \mathcal{L}_\mathcal{G} \nabla_{L^2} E(u). \tag{3.4}$$

Note that although the L^2 gradient is not always guaranteed to exist as an element of $L^2(\Omega)$, it is only necessary that $\nabla_{L^2} E(u) \in H^{-k}(\Omega)$ for (3.4) to hold.

3.2. Sobolev diffusion equations. As we have seen, a majority of the Sobolev gradients that we will be interested in can be written in the form $\nabla_\mathcal{G} E(u) = \mathcal{L}\mathcal{D}u$ where $\mathcal{L} : H^{-k}(\Omega) \to H_0^k(\Omega)$ is bounded and linear and $\mathcal{D} : H_0^k(\Omega) \to H^{-k}(\Omega)$ is a possibly non-linear differential operator. Thus, we will study the general class of differential equations given by

$$u(0) = u_0, \quad \frac{du}{dt} = \mathcal{L}\mathcal{D}u(t), \quad t \in (0, T] \tag{3.5}$$

where $u_0 : \Omega \to \mathbb{R}$ is the initial condition and $\mathcal{L}$ and $\mathcal{D}$ are as stated above. In image processing, u_0 is the image to be processed. Associated to (3.5) we have the following existence and uniqueness result which follows from the theory of ODE in Banach spaces [53, 9].

THEOREM 3.1. *Let X, Y be Banach spaces and $B : Y \to X$ be a bounded and linear operator. Suppose $A : X \to Y$ is a bounded and locally Lipschitz operator. Then for any $T > 0$ and $u_0 \in X$, there exists a unique $u \in C^1([0, T]; X)$ satisfying*

$$u(0) = u_0, \quad \frac{du}{dt} = BAu(t), \quad t \in (0, T]. \tag{3.6}$$

3.3. Generalized Perona–Malik equations. Motivated by the Perona–Malik and You–Kaveh equations, we consider the family of $2k$-order differential equations adapted from [31]

$$u(0) = u_0, \quad \frac{du}{dt} = \mathcal{L}\begin{cases} -\Delta^{k/2}\left(g(|\Delta^{k/2}u|^2)\Delta^{k/2}u\right), & k \text{ even} \\ \Delta^{(k-1)/2}\mathrm{div}\left(g(|\nabla\Delta^{(k-1)/2}u|^2)\nabla\Delta^{(k-1)/2}u\right), & k \text{ odd} \end{cases}. \tag{3.7}$$

THEOREM 3.2. *Let $k \in \mathbb{N}$ and $g : [0, \infty) \to \mathbb{R}$ be a bounded and continuously differentiable function satisfying*

$$|sg'(s)| \leq C, \quad s \in [0, \infty),$$

for some $C > 0$. Then for every $u_0 \in H^k(\Omega)$, there exists a unique $u \in C^1([0,T], H^k(\Omega))$ solving (3.7)*. Furthermore, if $u_0 \in H_0^k(\Omega)$ then $u(t) \in H_0^k(\Omega)$ for all $t \in (0,T]$.*

Proof. Let $F : \mathbb{R}^m \to \mathbb{R}^m$ be defined by $F(x) = g(|x|^2)x$, where $m \geq 1$. It follows from the fundamental theorem of calculus that

$$F(y) - F(x) = \int_0^1 DF((1-t)x + ty) \cdot (y - x)dt.$$

where DF denotes the Jacobian matrix of F. Thus we have the estimate

$$\frac{|F(x) - F(y)|}{|x - y|} \leq \sup_{z \in \mathbb{R}^m} \|DF(z)\|_{\mathcal{F}},$$

where $\|DF(x)\|_{\mathcal{F}}$ denotes the Frobenius norm of $DF(x)$. If $\|DF(x)\|_{\mathcal{F}}$ is uniformly bounded across all $x \in \mathbb{R}^m$, then it will follow that F is Lipschitz continuous. A short computation yields

$$DF(x) = \left(F^i_{x_j}\right)^j_i = \left(2g'(|x|^2)x_i x_j + \delta_{ij} g(|x|^2)\right)^j_i,$$

where δ_{ij} is the Kronecker delta. Hence, we can bound the Frobenius norm of $DF(x)$ by

$$\|DF(x)\|_{\mathcal{F}} \leq 2|g'(|x|^2)|\,|x|^2 + \sqrt{n} g(|x|^2).$$

Since $|sg'(s)|$ and $|g(s)|$ are uniformly bounded, it follows that $\|DF(x)\|_{\mathcal{F}}$ is uniformly bounded and hence $F : \mathbb{R}^m \to \mathbb{R}^m$ is Lipschitz continuous.

We must now consider two cases, depending on whether k is even or odd. If k is even, it follows from the Lipschitzness of F that

$$\begin{aligned}\|g(|\Delta^{k/2}u|^2)\Delta^{k/2}u - g(|\Delta^{k/2}v|^2)\Delta^{k/2}v\|_{L^2(\Omega)} &= \|F(\Delta^{k/2}u) - F(\Delta^{k/2}v)\|_{L^2(\Omega)} \\ &\leq C\|\Delta^{k/2}(u-v)\|_{L^2(\Omega)} \\ &\leq C\|u - v\|_{H^k(\Omega)}.\end{aligned}$$

Since $\Delta^{k/2} : L^2(\Omega) \to H^{-k}(\Omega)$ is bounded and linear, it follows that the mapping $\mathcal{D} : H^k(\Omega) \to H^{-k}(\Omega)$ defined by

$$\mathcal{D}u = -\Delta^{k/2}\left(g(|\Delta^{k/2}u|^2)\Delta^{k/2}u\right),$$

is Lipschitz and hence bounded. Hence the result follows from theorem 3.1 with $A = \mathcal{D}$, $B = \mathcal{L}$, $X = H^k(\Omega)$ and $Y = H^{-k}(\Omega)$.

If k is odd, then we have

$$\begin{aligned}&\|g(|\nabla\Delta^{(k-1)/2}u|^2)\nabla\Delta^{(k-1)/2}u - g(|\nabla\Delta^{(k-1)/2}v|^2)\nabla\Delta^{(k-1)/2}v\|_{L^2(\Omega;\mathbb{R}^n)} \\ &= \|F(\nabla\Delta^{(k-1)/2}u) - F(\nabla\Delta^{(k-1)/2}v)\|_{L^2(\Omega;\mathbb{R}^n)} \\ &\leq C\|\nabla\Delta^{(k-1)/2}(u-v)\|_{L^2(\Omega;\mathbb{R}^n)} \\ &\leq C\|u-v\|_{H^k(\Omega)}.\end{aligned}$$

Since $\Delta^{(k-1)/2}\mathrm{div} : L^2(\Omega;\mathbb{R}^n) \to H^{-k}(\Omega)$ is bounded and linear, it follows that $\mathcal{D} : H^k(\Omega) \to H^{-k}(\Omega)$ defined by

$$\mathcal{D}u = \Delta^{(k-1)/2}\mathrm{div}\left(g(|\nabla\Delta^{(k-1)/2}u|^2)\nabla\Delta^{(k-1)/2}u\right)$$

is Lipschitz and hence bounded and the result follows from theorem 3.1.

Since the range of $\mathcal{L}$ is $H_0^k(\Omega)$, if $u_0 \in H_0^k(\Omega)$, we can apply theorem 3.1 with $X = H_0^k(\Omega)$ and $Y = H^{-k}(\Omega)$ to obtain that $u(t) \in H_0^k(\Omega)$ for $t > 0$. ∎

As a remark, the restriction $|sg'(s)| \leq C$ is not all that restrictive. This property is satisfied by both of the Perona–Malik diffusion coefficients [41]

$$g(s) = \frac{1}{1 + s/K^2}, \quad \text{and} \quad g(s) = e^{-s/K^2}.$$

In image processing, it is commonplace to estimate the gradient of the image via a convolution with a Gaussian kernel [33]. This yields a robust estimation of the image gradient in the presence of noise. Such a technique has also been shown to regularize ill-posed diffusion equations such as the Perona–Malik equation [13, 2, 3]. It is therefore interesting to study the equations

$$u(0) = u_0, \quad \frac{du}{dt} = \mathcal{L} \begin{cases} -\Delta^{k/2}\left(g(|\Delta^{k/2}u_\sigma|^2)\Delta^{k/2}u\right), & k \text{ even} \\ \Delta^{(k-1)/2}\mathrm{div}\left(g(|\nabla\Delta^{(k-1)/2}u_\sigma|^2)\nabla\Delta^{(k-1)/2}u\right), & k \text{ odd} \end{cases}, \tag{3.8}$$

with initial condition $u(0) = u_0 \in H^k(\Omega)$. The notation used here is $u_\sigma \triangleq G_\sigma * \tilde{u}$ where $\tilde{u}$ is a bounded linear extension of u from $H^k(\Omega)$ to $L^2(\mathbb{R}^n)$ (i.e. there exists $C > 0$ such that $\|\tilde{u}\|_{L^2(\mathbb{R}^n)} \leq C\|u\|_{H^k(\Omega)}$ for all $u \in H^k(\Omega)$). A common choice for the extension operator is to extend u to be identically zero on $\mathbb{R}^n - \Omega$. Note that (3.8) cannot be interpreted as a gradient descent or ascent. Associated to the regularized diffusion PDE (3.8) we have the following theorem.

THEOREM 3.3. *Let $k \in \mathbb{N}$ and $g : \mathbb{R} \to \mathbb{R}$ be a function such that $s \mapsto g(s^2)$ is smooth, bounded and Lipschitz. Then for every $u_0 \in H^k(\Omega)$, there exists a unique $u \in C^1([0,T], H^k(\Omega))$ solving (3.8). Furthermore, if $u_0 \in H_0^k(\Omega)$ then $u(t) \in H_0^k(\Omega)$ for all $t \in [0,T]$.*

Proof. Let $F : H^k(\Omega) \to L^\infty(\Omega)$ be defined by

$$Fu = \begin{cases} g(|\Delta^{k/2}u_\sigma|^2), & k \text{ even} \\ g(|\nabla\Delta^{k/2}u_\sigma|^2), & k \text{ odd.} \end{cases}$$

Let us show that F is Lipschitz continuous. For k even, since $s \mapsto g(s^2)$ is Lipschitz, for $u, v \in H^k(\Omega)$ we have

$$\begin{aligned} \|Fu - Fv\|_{L^\infty(\Omega)} &= \sup_{x\in\Omega} \left| g(|(\Delta^{k/2}u_\sigma)(x)|^2) - g(|(\Delta^{k/2}v_\sigma)(x)|^2) \right| \\ &\leq \sup_{x\in\mathbb{R}^n} K \left| (\Delta^{k/2}G_\sigma) * (\tilde{u} - \tilde{v})(x) \right| \\ &\leq K\|\Delta^{k/2}G_\sigma\|_{L^\infty(\mathbb{R}^n)}\|\tilde{u} - \tilde{v}\|_{L^2(\mathbb{R}^n)}. \end{aligned}$$

For k odd, we have

$$\begin{aligned} \|Fu - Fv\|_{L^\infty(\Omega)} &= \sup_{x\in\Omega} \left| g(|(\nabla\Delta^{(k-1)/2}u_\sigma)(x)|^2) - g(|(\nabla\Delta^{(k-1)/2}v_\sigma)(x)|^2) \right| \\ &\leq \sup_{x\in\mathbb{R}^n} K \left| (\nabla\Delta^{(k-1)/2}G_\sigma) * (\tilde{u} - \tilde{v})(x) \right| \\ &\leq K\|\nabla\Delta^{(k-1)/2}G_\sigma\|_{L^\infty(\mathbb{R}^n;\mathbb{R}^n)}\|\tilde{u} - \tilde{v}\|_{L^2(\mathbb{R}^n)}. \end{aligned}$$

Since $u \mapsto \tilde{u}$ is a bounded linear extension from $H^k(\Omega)$ to $L^2(\mathbb{R}^n)$ we have

$$\|\tilde{u} - \tilde{v}\|_{L^2(\mathbb{R}^n)} \leq C\|u - v\|_{H^k(\Omega)},$$

and hence F is Lipschitz continuous.

Now, note that equation (3.8) can be written in the form

$$u(0) = u_0, \quad \frac{du}{dt} = \mathcal{L}\mathcal{D}u(t), \quad t > 0,$$

where $\mathcal{D} : H^k(\Omega) \to H^{-k}(\Omega)$ is given by

$$\mathcal{D}u = \sum_{|\alpha|,|\beta| \leq k} D^\beta(a_{\alpha,\beta}F(u)D^\alpha u),$$

and $a_{\alpha,\beta}$ are positive integers. Also note that

$$\begin{aligned}
&\|a_{\alpha,\beta}F(u)D^\alpha u - a_{\alpha,\beta}F(v)D^\alpha v\|_{L^2(\Omega)} \\
&\qquad \leq a_{\alpha,\beta}\|(F(u) - F(v))D^\alpha u\|_{L^2(\Omega)} + a_{\alpha,\beta}\|F(v)(D^\alpha u - D^\alpha v)\|_{L^2(\Omega)} \\
&\qquad \leq a_{\alpha,\beta}\|F(u) - F(v)\|_{L^\infty(\Omega)}\|u\|_{H^k(\Omega)} + a_{\alpha,\beta}\|F(v)\|_{L^\infty(\Omega)}\|u - v\|_{H^k(\Omega)}.
\end{aligned}$$

Hence $\mathcal{D}$ is locally Lipschitz. Since g is bounded, $\mathcal{D}$ is bounded, and we can apply the result from theorem 3.1. As in the proof of theorem 3.2, if $u_0 \in H_0^k(\Omega)$, then $u(t) \in H_0^k(\Omega)$ for all $t > 0$. □

PROPOSITION 3.4. *Let $\mathcal{G}$ be an inner product on $H_0^k(\Omega)$ which induces a norm equivalent to the standard norm, and let $u \in C^1([0,T]; H_0^k(\Omega))$ be a solution to* (3.7) *of order $2k$ with initial condition $u_0 \in H_0^k(\Omega)$ and $\mathcal{L} = \mathcal{L}_\mathcal{G}$. If g is non-negative, then $t \mapsto \mathcal{G}(u(t), u(t))$ is monotonically decreasing. The same result holds if u is a solution of* (3.8).

Proof. We will prove the proposition for k even, the odd case being identical. Let $u \in C^1([0,T]; H_0^k(\Omega))$ be a solution of (3.7) with k odd and g non-negative. Then, integrating by parts yields

$$\begin{aligned}
\frac{1}{2}\frac{d}{dt}\mathcal{G}(u(t), u(t)) &= \mathcal{G}\left(\frac{du}{dt}(t), u(t)\right) \\
&= -\mathcal{G}\left(\mathcal{L}_\mathcal{G}\Delta^{k/2}\left(g(|\Delta^{k/2}u(t)|)\Delta^{k/2}u(t)\right), u(t)\right) \\
&= -\left\langle \Delta^{k/2}\left(g(|\Delta^{k/2}u(t)|)\Delta^{k/2}u(t)\right), u(t)\right\rangle_{H^{-k}, H_0^k} \\
&= -\int_\Omega g(|\Delta^{k/2}u|)|\Delta^{k/2}u(t)|^2 dx \\
&\leq 0.
\end{aligned}$$

□

3.4. Sobolev inner products. We will now introduce a particular family of inner products which have appeared previously in [11]. Consider first that to compute a Sobolev gradient with respect to an arbitrary inner product $\mathcal{G}$, one must be able to compute the operator $\mathcal{L}_\mathcal{G}$ defined in (3.3). For an arbitrary inner product this amounts to solving a $2k$-order PDE which may be a difficult numerical problem. Thus, we should choose a family of inner products which yield tractable differential

equations, ones which we can easily compute the Green's function for. On $H_0^1(\Omega)$, we consider the inner products $\mathcal{G}_{1,\lambda} : H_0^1(\Omega) \times H_0^1(\Omega) \to \mathbb{R}$ defined by

$$\mathcal{G}_{1,\lambda}(u,v) = \int_\Omega uv + \lambda(\nabla u \cdot \nabla v)dx, \tag{3.9}$$

where $\lambda > 0$. Then integration by parts yields

$$\mathcal{G}_{1,\lambda}(u,v) = \langle (I - \lambda\Delta)u, v\rangle_{H^{-1},H_0^1}.$$

where I denotes the identity operator and $u, v \in H_0^1(\Omega)$. Hence, applying the operator $\mathcal{L}_{\mathcal{G}_{1,\lambda}}$ to an element $u \in H^{-1}(\Omega)$ amounts to solving the elliptic PDE

$$\begin{cases} (I - \lambda\Delta)\mathcal{L}_{\mathcal{G}_{1,\lambda}} u = u, & \text{in } \Omega \\ \mathcal{L}_{\mathcal{G}_{1,\lambda}} u = 0, & \text{on } \partial\Omega, \end{cases} \tag{3.10}$$

in the distributional sense. For the domain $\Omega = \mathbb{R}^n$ the Green's function for (3.10) is a rescaled Bessel potential [21] and efficient numerical schemes can be used to compute the solution [10, 11]. We will use the notation

$$\mathcal{L}_{\mathcal{G}_{1,\lambda}} = (I - \lambda\Delta)^{-1}, \tag{3.11}$$

to mean that $\mathcal{L}_{\mathcal{G}_{1,\lambda}} u$ satisfies (3.10) for $u \in H_0^1(\Omega)$.

Analogously, for $H_0^k(\Omega)$ one can define a family of inner products $\mathcal{G}_{k,\lambda} : H_0^k(\Omega) \times H_0^k(\Omega) \to \mathbb{R}$ of the form

$$\mathcal{G}_{k,\lambda}(u,v) = \int_\Omega \sum_{|\alpha|\le k} b_\alpha D^\alpha u D^\alpha v dx, \tag{3.12}$$

where b_α are positive integers chosen so that upon integration by parts, one has

$$\mathcal{G}_{k,\lambda}(u,v) = \langle (I - \lambda\Delta)^k u, v\rangle_{H^{-k},H_0^k},$$

for $u, v \in H_0^k(\Omega)$. Similarly to the first order case, we will use the notation

$$\mathcal{L}_{\mathcal{G}_{k,\lambda}} = (I - \lambda\Delta)^{-k}, \tag{3.13}$$

to mean that $\mathcal{L}_{\mathcal{G}_{k,\lambda}} u$ solves the k^{th} order analog of (3.10). For $\Omega = \mathbb{R}^n$, the Green's function corresponding to $(I - \lambda\Delta)^{-k}$ can be computed and (3.13) reduces to a convolution operator which is a common operation in image processing. See section 5 for details. As an example, the gradient descent equation on PM_ϕ with respect to the inner product $\mathcal{G}_{k,\lambda}$ is

$$u(0) = u_0, \quad \frac{du}{dt} = (I - \lambda\Delta)^{-k}\mathrm{div}(\phi'(|\nabla u|^2)\nabla u), \quad t > 0.$$

3.5. Limiting cases. Consider the second order Perona–Malik equation

$$u(0) = u_0, \quad \frac{du}{dt} = \mathrm{div}(g(|\nabla u|^2)\nabla u), \quad t > 0 \tag{3.14}$$

and the Sobolev gradient descent Perona–Malik equation

$$u(0) = u_0, \quad \frac{du}{dt} = (I - \lambda\Delta)^{-1}\mathrm{div}(g(|\nabla u|^2)\nabla u), \quad t > 0 \tag{3.15}$$

An interesting question at this point concerns the limiting behaviour of (3.15) as $\lambda \to 0^+$, so consider a sequence $\{u_k\}_{k=1}^{\infty}$ where $u_k \in C^1([0,T]; H_0^1(\Omega))$ is the unique solution of (3.15) with $\lambda = 1/k$. It follows from proposition 3.4 that the sequence u_k is uniformly bounded in $L^2([0,T]; L^2(\Omega))$, so by passing to a subsequence if necessary, we have the existence of $u \in L^2([0,T]; L^2(\Omega))$ such that $u_k \rightharpoonup u$. The difficulty comes in getting an analogous bound on the gradients of the sequence. To see this, we can consider the typical Perona–Malik potential function $\phi(s) = \ln(1+s)$. Then each u_k would satisfy

$$\int_\Omega \phi(|\nabla u_k(t)|^2)dx \leq \int_\Omega \phi(|\nabla u_0|^2)dx.$$

Since ϕ is non-convex and has sublinear growth, the functional $E[u] = \int_\Omega \phi(|\nabla u|^2)dx$ is not coercive and hence the above inequality does not imply any kind of bound on the ∇u_k.

In fact, it is not hard to see that there exist sequences u_n with $\|u_n\|_{H^1} \to \infty$ but $E[u_n] \to 0$. Take for instance $\Omega = (-1,1)$ and

$$u_n(x) = \begin{cases} 0, & -1 < x < 0, \\ nx, & 0 \leq x \leq 1/n, \\ 1, & 1/n < x < 1. \end{cases} \tag{3.16}$$

Then $\|u_n\|^2_{H^1(\Omega)} \geq n$ and $E[u_n] = \ln(1+n^2)/n$. Hence we obtain that $\|u_n\|_{H^1(\Omega)} \to \infty$ and $E[u_n] \to 0$. In a certain sense, this behaviour is expected from the Perona–Malik functional. The sequence u_n is approaching a step discontinuity at $x = 0$ and it is well-known that the Perona–Malik equation can sharpen edges and create discontinuities (called staircasing) in smooth regions of an image. Hence we should not expect our sequence $u_k \rightharpoonup u$ to have a bounded gradient. We should expect it to develop singularities in the gradient, such as in the example above. This suggests that the limit u would have have to be interpreted as a measure valued solution to (3.14) if anything. An interesting extension of this work would be to study this limiting sequence in comparison to other works on measure-valued solutions to Perona–Malik type equations [46, 15].

4. Anisotropic image sharpening. In this section we propose some non-linear well-posed sharpening techniques based on gradient flows on a Perona–Malik style energy functional $PM_\phi : H_0^1(\Omega) \to \mathbb{R}$ defined by

$$PM_\phi[u] = \int_\Omega \phi(|\nabla u|^2). \tag{4.1}$$

For the case of image diffusion (gradient descent on (4.1)), Perona and Malik [41] proposed the functions $\phi(s) = \ln(1+s)$ and $\phi(s) = 1 - e^{-s}$. The TV approach corresponds to $\phi(s) = \sqrt{s}$. In each of these examples, the potential ϕ is (A) concave and (B) has sub-linear growth. (A) encourages the smoothing of fine details while (B) prevents the smoothing of strong edges. For the case of image sharpening (gradient ascent on (4.1)), what type of potential ϕ should we use? First we should decide what properties are desirable in a sharpening algorithm. Intuitively, we want the algorithm to sharpen relevant features in the images such as edges while inhibiting the sharpening of fine details which may be interpreted as noise. Thus we are looking for a ϕ with the following properties:

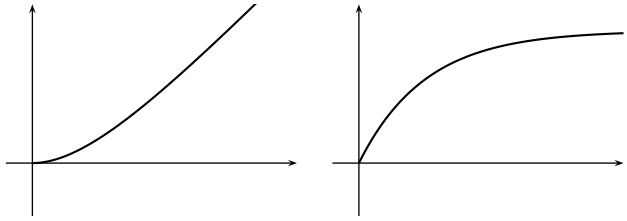

(a) $\phi(s)$ (b) $g(s) = \phi'(s)$

FIG. 4.1. *The qualitative properties of (a) the sharpening potential $\phi(s)$ and (b) the diffusion coefficient, $g(s) = \phi'(s)$.*

- ϕ should be convex (near zero),
- ϕ should have at least linear growth.

Since the diffusion coefficient $g(s) = \phi'(s)$ must be bounded in order to apply the existence and uniqueness results, we will look for a ϕ which has linear growth. If we do not ask that ϕ is strictly convex, then $\phi(x) = x$ would be a candidate. We call this isotropic sharpening and it has been studied previously in [10, 11]. Isotropic sharpening sharpens all gradients equally and hence has the effect of enhancing noise as well as image features. Thus we should search for a ϕ which is more convex near the origin. Figure 4.1 shows the qualitative properties of such a ϕ. We will use the function ϕ defined by

$$\phi(s) = s - (1 - e^{-s}). \tag{4.2}$$

For this choice of ϕ, the diffusion coefficient is given by $g(s) = \phi'(s) = 1 - e^{-s}$. Hence, we propose the following anisotropic equation for image sharpening

$$u(0) = u_0, \quad \frac{du}{dt} = -(I - \lambda\Delta)^{-1}\mathrm{div}(g(|\nabla u|^2)\nabla u), \quad t > 0 \tag{4.3}$$

where the diffusion coefficient for g is given by

$$g(s) = 1 - e^{-s/K^2}. \tag{4.4}$$

The threshold $K > 0$ determines which details in the image are sharpened (in terms of the magnitude of ∇u). One can set

$$K = \alpha \left(\int_\Omega |\nabla u_0|^2 \right)^{1/2},$$

where $\alpha > 0$ is a proportionality constant. We have found that $\alpha = 1$ works well for clean natural images. In the presence of noise, one must increase α to avoid enhancing the noise as well. The amount by which α should be increased will depend on the noise properties. In these simple experiments we have set $\alpha = 2$ for noisy images.

It is interesting to note that since the diffusion coefficient g is a linear combination of isotropic and anisotropic terms, (4.3) can be expanded into the sum of the corresponding isotropic and anisotropic diffusion terms. Thus anisotropic sharpening with this particular functional can also be viewed as a combination of isotropic sharpening and anisotropic smoothing. However, since ϕ is always increasing, the resulting effect of this combination is truly an anisotropic sharpening; i.e. there is no

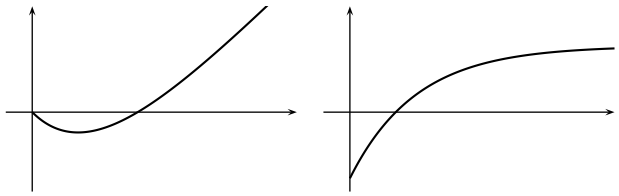

(a) $\phi(s)$ (b) $g(s) = \phi'(s)$

FIG. 4.2. *The qualitative properties of (a) the combined smoothing/sharpening potential $\phi(s)$ and (b) the diffusion coefficient, $g(s) = \phi'(s)$.*

smoothing, only less sharpening of weaker gradients. We could, however add a weight to the anisotropic term to obtain a combined smoothing and sharpening model. For example, consider the smoothing/sharpening potential

$$\phi(s) = s - \beta(1 - e^{-s}), \tag{4.5}$$

which yields the diffusion coefficient

$$g(s) = 1 - \beta e^{-s/K^2}. \tag{4.6}$$

We will call this model the anisotropic smoothing/sharpening model. The parameter $\beta > 0$ controls the amount of sharpening. If $\beta > 1$, then ϕ is initially decreasing and negative but still attains linear growth for larger gradients. This yields smoothing of weak gradients and sharpening of stronger gradients. See figure 4.2 for the qualitative properties of the combined smoothing/sharpening potential.

We should note that, contrary to many works on image restoration, we do not include a data fidelity term in our sharpening model. This is because, when equipped with the standard fidelities (e.g., L^2 or L^1 distance), the gradient flows that we have proposed will *not* converge to minimizers of the fidelity augmented functionals. As such, adding a fidelity term will serve little purpose as one would still need to select a stopping time independent of the fidelity. As an example, consider constraining the isotropic sharpening functional with an L^2 fidelity:

$$E[u] = -\frac{1}{2}\int_\Omega |\nabla u|^2\,dx + \frac{1}{2}\int_\Omega (u - u_0)^2\,dx.$$

It is not hard to see that E does not admit a minimizer, and hence the fidelity cannot be used to provide a stopping condition for the sharpening PDE.

5. Numerical Implementation. We will work on a grid of size $N_1 \times \cdots \times N_n$ and assume that the sampling period along axis i is h_i. An image u is then a mapping $(\ell_1, \ldots, \ell_n) \mapsto u(\ell_1, \ldots, \ell_n)$. Let $D^+_{x_i}$ and $D^-_{x_i}$ denote the forward and backward difference quotients defined by

$$D^+_{x_i} u(\ell_1, \ldots, \ell_n) = \frac{1}{h_i}(u(\ell_1, \ldots, \ell_i + 1, \ldots, \ell_n) - u(\ell_1, \ldots, \ell_i, \ell_n)),$$

and

$$D^-_{x_i} u(\ell_1, \ldots, \ell_n) = \frac{1}{h_i}(u(\ell_1, \ldots, \ell_i, \ldots, \ell_n) - u(\ell_1, \ldots, \ell_i + 1, \ell_n)).$$

$$10^{-3} \times \begin{bmatrix} 0.61700 & 0.55367 & 0.40523 & 0.24979 & 0.13474 & 0.06585 \\ 1.86521 & 1.62596 & 1.10380 & 0.61740 & 0.30170 & \\ 5.80472 & 4.81757 & 2.90906 & 1.42427 & & \\ 19.01402 & 14.29655 & 7.09452 & & & \\ 69.80074 & 40.13533 & & & & \\ 201.79638 & & & & & \end{bmatrix}$$

(a) $k = 1, \lambda = 1$

$$10^{-3} \times \begin{bmatrix} 0.50476 & 0.44298 & 0.30343 & 0.16783 & 0.07815 & 0.03187 \\ 1.86883 & 1.59315 & 1.01090 & 0.50529 & 0.21165 & \\ 6.72481 & 5.48020 & 3.11355 & 1.36485 & & \\ 23.01362 & 17.34795 & 8.35586 & & & \\ 70.21128 & 45.38850 & & & & \\ 128.94840 & & & & & \end{bmatrix}$$

(b) $k = 2, \lambda = 1/2$

$$10^{-3} \times \begin{bmatrix} 0.43778 & 0.37876 & 0.24857 & 0.12806 & 0.05407 & 0.01951 \\ 1.83869 & 1.54655 & 0.94152 & 0.43838 & 0.16615 & \\ 7.17922 & 5.79592 & 3.18416 & 1.30718 & & \\ 24.86272 & 18.84026 & 8.99075 & & & \\ 68.29509 & 46.88325 & & & & \\ 107.62864 & & & & & \end{bmatrix}$$

(c) $k = 3, \lambda = 1/3$

FIG. 5.1. *Discrete approximations to the Sobolev kernels $S_{k,\lambda}$ for (a) $k = 1, \lambda = 1$, (b) $k = 2, \lambda = 1/2$, and (c) $k = 3, \lambda = 1/3$. Note that each convolution kernel is 11×11. Since the kernels are rotational symmetric, we have only displayed the non-redundant coefficients here.*

We use the following standard discretizations:

$$u_{x_i} = \frac{1}{2}(D^+_{x_i} + D^-_{x_i})u \tag{5.1}$$

$$u_{x_i x_j} = \frac{1}{4}(D^+_{x_i} D^+_{x_j} + D^+_{x_i} D^-_{x_j} + D^-_{x_i} D^+_{x_j} + D^-_{x_i} D^-_{x_j})u, \quad i \neq j \tag{5.2}$$

$$u_{x_i x_i} = D^+_{x_i} D^-_{x_i} u \tag{5.3}$$

$$\Delta u = \sum_{i=1}^{n} D^+_{x_i} D^-_{x_i} u \tag{5.4}$$

We discretize the Perona–Malik style divergence form operator by expanding it formally as

$$\operatorname{div}(g(|\nabla u|^2)\nabla u) = g(|\nabla u|^2)\Delta u + 2g'(|\nabla u|^2) \sum_{i,j=1}^{n} u_{x_i} u_{x_j} u_{x_i x_j}.$$

Given a differential equation $du/dt = Au$, we use the standard time-evolution discretization

$$u^{n+1} = u^n + \delta t A u^n,$$

where δt should satisfy the stability condition

$$\delta t \max(|Au^n|) \leq 2.5$$

We discretize the operator $(I - \lambda\Delta)^{-k}$ by computing a discrete approximation to the Green's function [10, 11]. The Green's function for the domain $\Omega = \mathbb{R}^n$ is a type of rescaled Bessel function [11]

$$S_{k,\lambda}(x) = \frac{1}{(k-1)!(4\pi\lambda)^{n/2}} \int_0^\infty \frac{e^{-t-\frac{|x|^2}{4t\lambda}}}{t^{n/2-(k-1)}} dt. \tag{5.5}$$

The operator $\mathcal{L}_{\mathcal{G}_{k,\lambda}} = (I - \lambda\Delta)^{-k}$ can be computed via the convolution

$$\mathcal{L}_{\mathcal{G}_{k,\lambda}} u = (I - \lambda\Delta)^{-k} u = S_{k,\lambda} * u.$$

Since the Green's function $S_{k,\lambda}$ may have a singularity at the origin (depending on the values of k, λ and the dimension n) the discrete approximation must be done carefully [10, 11]. An accurate and computationally efficient method is to average the kernel $S_{k,\lambda}$ around each image pixel and use the averaged values as the discrete approximation. This method has been proven to converge to the continuous convolution as the sampling period tends to zero [10]. The convolution kernels obtained with this method are shown in figure 5.1 for $k = 1, 2, 3$ and $\lambda = 1, 1/2, 1/3$ respectively. Each of the convolution kernels is 11×11; only the non-redundant coefficients are displayed. For images with bounded domains (e.g., $[0, 1]^2$) we reflect the image about its boundary and then periodically extend the image to $\mathbb{R}^n$ in order to compute the convolution. In practice, since the kernel is 11×11 pixels, it is only necessary to reflect the image about its boundary.

6. Experimental results. The selection of a stopping time is an important consideration in this framework. For this, we consider the fact that the functional $E_s[u] = \int_\Omega |\nabla u|^2$ is a measure of the sharpness of the image u. As motivation for this choice of sharpness measure, note that Gaussian blurring can be interpreted as gradient descent on E_s. Instead of selecting a stopping time, we select a sharpness factor $\alpha > 1$, and the PDE is run until $E_s[u]/E_s[u_0] = \alpha$, where u_0 is the initial image to be processed. Typically, one can choose $\alpha \in [2, 5]$ to obtain good sharpening. In our experiments, we have used sharpness factors of 3 and 4.

Figure 6.1 compares anisotropic sharpening (4.3), isotropic sharpening, and the shock filter on the lena test image. The isotropic and anisotropic sharpening were each run until the functional $u \mapsto \int_\Omega |\nabla u|^2$ was tripled. The shock filter was run until convergence. We can see from figure 6.1 that the isotropic sharpening does a good job of sharpening the texture in the hair and hat and some of the sharp edges. However, isotropic diffusion also enhances the background noise on her face and in the background beside the hat. In comparison, the anisotropic sharpening only enhances important features, such as the hair and strong edges while keeping the noise in the background. It actually appears that the anisotropic sharpening is slightly smoothing some of the light noise on her face. When we compare with the shock filter in figure 6.1, we see that anisotropic sharpening, in similar fashion to isotropic sharpening, yields a more natural looking image and acts to enhance local maximums and minimums while the shock filter produces a cartoon-like piecewise constant image with sharp boundaries. In figure 6.2 we applied a Gaussian blur to the nature image and show the results of anisotropic sharpening. We see very similar results as with the lena test

(a) Original (b) Anisotropic Sobolev Sharpening

(c) Isotropic Sobolev Sharpening (d) Shock Filter

FIG. 6.1. *Comparison between (b) anisotropic Sobolev sharpening, (c) isotropic Sobolev sharpening and (d) the shock filter, all applied to (a) the lena test image. The anisotropic and isotropic sharpening algorithms were run until the functional* $u \mapsto \int_\Omega |\nabla u|^2$ *was increase to three times its original value.*

image. The sharpening algorithm does not attempt to bring back fine details that were destroyed in the blurring process.

To further explore the robustness with respect to noise, in figure 6.3, we compare isotropic and anisotropic sharpening to the combined anisotropic sharpening and smoothing model on a corrupted version of the baboon image. We have corrupted the

(a) Gaussian blurred original

(b) Anisotropic Sobolev sharpening

FIG. 6.2. *Example of anisotropic Sobolev sharpening on a Gaussian blurred test image. The PDE was run until the functional* $u \mapsto \int_\Omega |\nabla u|^2$ *was increased to three times its original value.*

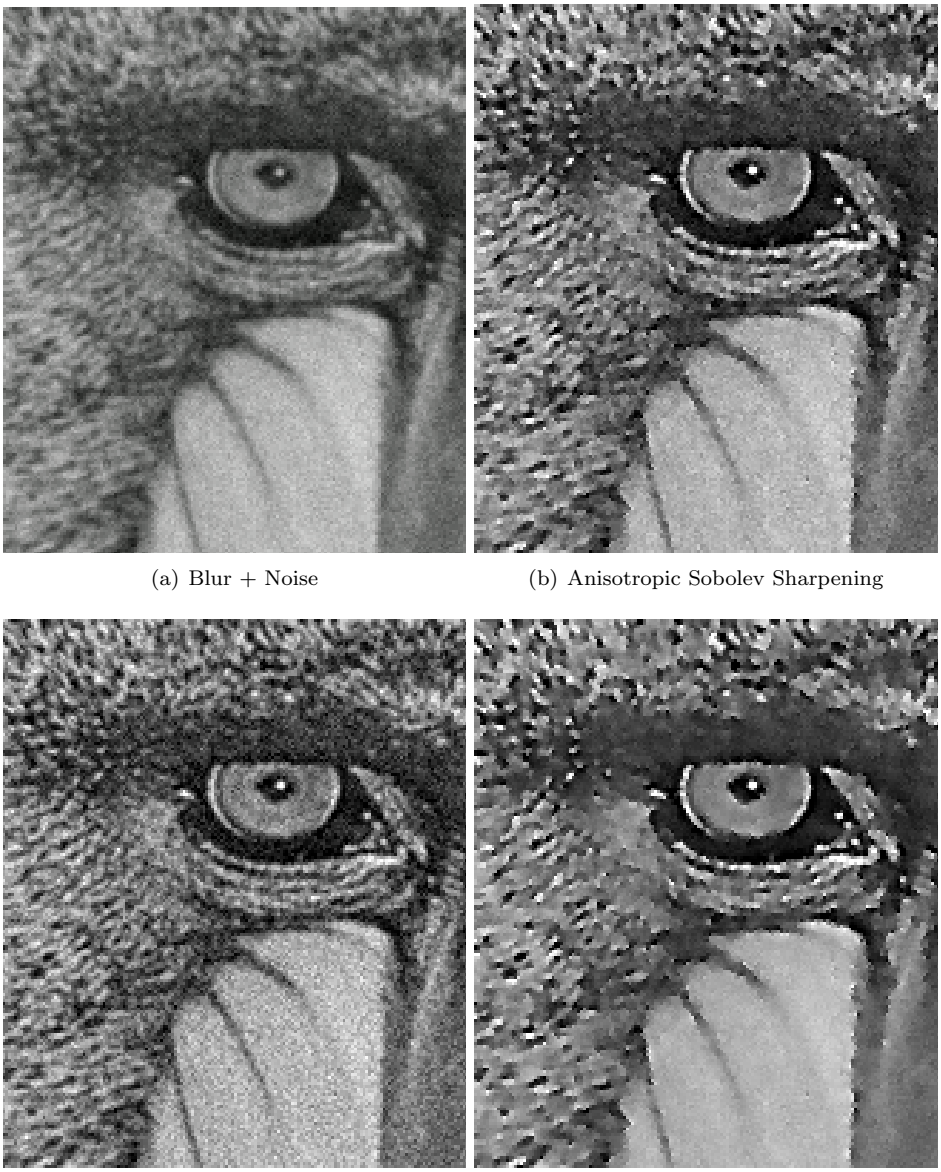

(a) Blur + Noise

(b) Anisotropic Sobolev Sharpening

(c) Isotropic Sobolev Sharpening

(d) Anisotropic Sobolev Sharpening/Smoothing with $\beta = 1.2$

FIG. 6.3. *Comparison between (b) anisotropic Sobolev sharpening, (c) isotropic Sobolev sharpening and (d) the shock filter, all applied to (a) the baboon test image corrupted with Gaussian blur and additive Gaussian noise. The anisotropic and isotropic sharpening algorithms were run until the functional* $u \mapsto \int_\Omega |\nabla u|^2$ *was increase to four times its original value.*

image by first applying a Gaussian blur and then additive Gaussian noise. Although the noise is quite faint, we can see that the isotropic sharpening algorithm enhances it quite a bit. As we expected from our experiments with lena, the anisotropic sharpening algorithm is much more robust in the presence of noise. We can see from figure 6.3 that the anisotropic sharpening neither smoothes nor enhances the noise; it more

or less keeps the same noise level while sharpening more global features, such as the eyes and the texture on the face. The combined sharpening/smoothing algorithm, on the other hand, is able to remove the noise and sharpen edges and features at the same time.

7. Conclusion and future work. We have proposed a new family of well-posed image diffusion and sharpening algorithms obtained via Sobolev gradient descent and ascent on the traditional anisotropic diffusion functionals. The well-posedeness of these new gradient flows opens the door to a wide variety of sharpening and diffusion techniques which were previously impossible under L^2 gradient descent. We showed how one could easily use this new framework to design a sharpening PDE which performs well even in the presence of noise. We further showed how one could slightly modify the anisotropic sharpening PDE to obtain a combined sharpening and smoothing PDE. It should be emphasized that we have only scratched the surface of what is possible with this new image diffusion/sharpening framework. It would be interesting to experiment with the higher order anisotropic sharpening algorithms, such as the You–Kaveh model and the higher order generalizations. We are currently investigating these higher order PDE as well as sharpening algorithms where the diffusion coefficient depends not only on the gradient, but also on higher order derivatives of the image. It is likely that such a descriptor could better distinguish edges from noise and allow the sharpening algorithms to perform well in the presence of even higher noise levels. We have also shown how one can perturb the Perona–Malik equation to obtain a well-posed PDE while retaining the gradient descent property. It would be interesting to understand more about the connection between these perturbed equations and the ill-posed Perona–Malik equation.

8. Acknowledgments. A. Mansouri was partially supported by a research grant from the Natural Science and Engineering Research Council of Canada (NSERC).

REFERENCES

[1] L. Alvarez, F. Guichard, P.-L. Lions, and J.-M. Morel, *Axioms and fundamental equations of image processing*, Archive for Rational Mechanics and Analysis, 123 (1993), pp. 199–257.
[2] L. Alvarez, P.-L. Lions, and J.-M. Morel, *Image selective smoothing and edge detection by nonlinear diffusion. II*, SIAM Journal of Numerical Analysis, 29 (1992), pp. 845–866.
[3] L. Alvarez and L. Mazorra, *Signal and image restoration using shock filters and anisotropic diffusion*, SIAM Journal on Numerical Analysis, 31 (1994), pp. 590–605.
[4] G. Aubert and P. Kornprobst, *Mathematical Problems in Image Processing: Partial Differential Equations and the Calculus of Variations*, Springer, Applied Mathematical Sciences, 2006.
[5] J.-F. Aujol, G. Aubert, L. Blanc-Féraud, and A. Chambolle, *Image decomposition into a bounded variation component and an oscillating component*, Journal of Mathematical Imaging Vision, 22 (2005), pp. 71–78.
[6] G. Bellettini and G. Fusco, *A regularized Perona-Malik functional: some aspects of the gradient dynamics.* unpublished, 2004.
[7] ———, *The Γ-limit and the related gradient flow for singular perturbation functionals of Perona-Malik type*, Transactions of the American Mathematical Society, 360 (2008), pp. 4929–4987.
[8] A. Braides, *Gamma-Convergence for Beginners*, Clarendon Press, September 2002.
[9] H. Brezis, *Analyse fonctionnelle : Théorie et applications*, Editions Masson, Paris, 1993.
[10] J. Calder, A. Mansouri, and A. Yezzi, *Image sharpening via Sobolev gradient flows*, SIAM Journal on Imaging Science, 3 (2010), pp. 981–1014.
[11] ———, *New possibilities in image diffusion via high-order Sobolev gradient flows*, Journal of Mathematical Imaging and Vision, (2011). To appear.
[12] C. Castaing, P. Raynaud de Fitte, and M. Valadier, *Young Measures on Topological*

Spaces With Applications in Control Theory and Probability Theory, Mathematics and Its Applications, Kluwer Academic Publishers, August 2004.

[13] F. Catté, P.-L. Lions, J.-M. Morel, and T. Coll, *Image selective smoothing and edge detection by nonlinear diffusion*, SIAM Journal on Numerical Analysis, 29 (1992), pp. 182–193.

[14] G. Charpiat, P. Maurel, J.-P. Pons, R. Keriven, and O. Faugeras, *Generalized gradients: Priors on minimization flows*, International Journal of Computer Vision, 73 (2007), pp. 325–344.

[15] Y. Chen and K. Zhang, *Young measure solutions of the two-dimensional Perona-Malik equation in image processing*, Communications on Pure and Applied Analysis, 5 (2006), pp. 617–637.

[16] G. Dal Maso, *An introduction to* Γ*-convergence*, Birkhauser Boston, 1993.

[17] S. Demoulini, *Young measure solutions for a nonlinear parabolic equation of forward-backward type*, SIAM Journal on Mathematical Analysis, 27 (1996), pp. 376–403.

[18] S. Esedoḡlu, *An analysis of the Perona-Malik scheme*, PhD thesis, Courant Institute of Mathematical Sciences, New York University, New York, NY, USA, 2000. Adviser-Kohn, Robert V.

[19] ———, *An analysis of the Perona-Malik scheme*, Communications on Pure and Applied Analysis, LIV (2001), pp. 0001–0046.

[20] ———, *Stability properties of the Perona–Malik scheme*, SIAM Journal on Numerical Analysis, 44 (2006), pp. 1297–1313.

[21] L.C. Evans, *Partial Differential Equations (Graduate Studies in Mathematics, V. 19) GSM/19*, American Mathematical Society, June 1998.

[22] M. Ghisi and M. Gobbino, *Gradient estimates for the Perona-Malik equation*, Mathematische Annalen, 337 (2007), pp. 557–590.

[23] ———, *A class of local classical solutions for the one-dimensional Perona-Malik equation*, Transactions of the American Mathematical Society, 361 (2009), pp. 6429–6446.

[24] G. Gilboa, N. Sochen, and Y.Y. Zeevi, *Forward-and-backward diffusion processes for adaptive image enhancement and denoising*, IEEE Transactions on Image Processing, 11 (2002), pp. 689–703.

[25] M. Gobbino, *Entire solutions of the one-dimensional Perona-Malik equation*, Communications in Partial Differential Equations, 32 (2007), pp. 719–743.

[26] J. B. Greer and A. L. Bertozzi, *Traveling wave solutions of fourth order PDEs for image processing*, SIAM Journal on Mathematical Analysis, 36 (2004), pp. 38–68.

[27] K. Hollig, *Existence of infinitely many solutions for a forward backward heat equation*, Transactions of the American Mathematical Society, 278 (1983), pp. 299–316.

[28] W.B. Richardson Jr., *High-order sobolev preconditioning*, Nonlinear Analysis, 63 (2005), pp. e1779–e1787. Invited Talks from the Fourth World Congress of Nonlinear Analysts (WCNA 2004).

[29] ———, *Sobolev gradient preconditioning for image-processing pdes*, Communications in Numerical Methods in Engineering, 24 (2008), pp. 493–504.

[30] S. Kichenassamy, *The Perona-Malik paradox*, SIAM Journal on Applied Mathematics, 57 (1997), pp. 1328–1342.

[31] C. Kublik, *Coarsening in high order, discrete, ill-posed diffusion equations*, Communications in Mathematical Sciences, 8 (2010), pp. 797–834.

[32] L.H. Lieu and L.A. Vese, *Image restoration and decomposition via bounded total variation and negative hilbert-sobolev spaces*, Applied Mathematics and Optimization, 58 (2008), pp. 167–193.

[33] D. Marr and E. Hildreth, *Theory of edge detection*, in Proceedings of the Royal Society of London, vol. 207 of Series B, Biological Sciences, Royal Society, Feb. 1980, pp. 187–217.

[34] Y. Meyer, *Oscillating patterns in image processing and nonlinear evolution equations*, The fifteenth Dean Jacqueline B. Lewis Memorial Lectures, American Mathematical Society, 2001.

[35] M. Morini, M. Negri, and G. Dal Maso, *Mumford-Shah functional as* Γ*-limit of discrete Perona-Malik energies*, Mathematical Models and Methods in Applied Sciences, 13 (2003), pp. 785–805.

[36] D. Mumford and J. Shah, *Boundary detection by minimizing functionals i*, in Proceedings of the IEEE Conference on Computer Vision and Pattern Recognition, 1985.

[37] J.W. Neuberger, *Sobolev Gradients and Differential Equations*, Lecture Notes in Mathematics, Springer Berlin / Heidelberg, 2nd ed., 2010.

[38] S. Osher and L. Rudin, *Feature-oriented image enhancement using shock filters*, SIAM Journal on Numerical Analysis, 27 (1990), pp. 919–940.

[39] ———, *Shocks and other nonlinear filtering applied to image processing*, Applications of Digital Image Processing XIV, 1567 (1991), pp. 414–431.
[40] V. Padrón, *Sobolev regularization of a nonlinear ill-posed parabolic problem as a model for aggregating populations*, Communications in Partial Differential Equations, 23 (1998), pp. 457–486.
[41] P. Perona and J. Malik, *Scale-space and edge detection using anisotropic diffusion*, IEEE Transactions on Pattern Analysis and Machine Intelligence, 12 (1990), pp. 629–639.
[42] L. Rudin, S. Osher, and E. Fatemi, *Nonlinear total variation based noise removal algorithms*, Physica D, 60 (1992), pp. 259–268.
[43] G. Sundaramoorthi, J.D. Jackson, and A. Yezzi, *Tracking with Sobolev active contours*, in In Proceedings Computer Vision and Pattern Recognition, 2006, pp. 674–680.
[44] G. Sundaramoorthi, A. Yezzi, and A.C. Mennucci, *Sobolev active contours*, International Journal of Computer Vision, 73 (2005), pp. 109–120.
[45] G. Sundaramoorthi, A. Yezzi, A.C. Mennucci, and G. Sapiro, *New possibilities with Sobolev active contours*, in In Scale Space Variational Methods, Springer-Verlag, 2007, pp. 153–164.
[46] S. Taheri, Q. Tang, and K. Zhang, *Young measure solutions and instability of the one-dimensional Perona-Malik equation*, Journal of Mathematical Analysis and Applications, 308 (2005), pp. 467–490.
[47] J. Weickert, *Anisotropic diffusion in image processing*, PhD thesis, University of Kaiserslautern, Germany, 1996.
[48] ———, *Anisotropic diffusion in image processing*, ECMI Series, Teubner-Verlag, Stuttgart, Germany, 1998.
[49] ———, *Coherence-enhancing diffusion filtering*, International Journal of Computer Vision, 31 (1999), pp. 111–127.
[50] M. Welk, G. Gilboa, and J. Weickert, *Theoretical foundations for discrete forward-and-backward diffusion filtering*, in Proceedings of the Second International Conference on Scale Space and Variational Methods in Computer Vision, Berlin, Heidelberg, 2009, Springer-Verlag, pp. 527–538.
[51] J. Yin and C. Wang, *Young measure solutions of a class of forward-backward diffusion equations*, Journal of Mathematical Analysis and Applications, 279 (2003), pp. 659–683.
[52] Y. You and M. Kaveh, *Fourth-order partial differential equations for noise removal*, IEEE Transactions on Image Processing, 9 (2000), pp. 1723–1730.
[53] E. Zeidler, *Nonlinear Functional Analysis and Its Applications: Pt. 1: Fixed-point Theorems*, Springer-Verlag New York Berlin Heidelbert Tokyo, 1986.
[54] K. Zhang, *Existence of infinitely many solutions for the one-dimensional Perona-Malik model*, Calculus of Variations and Partial Differential Equations, 26 (2006), pp. 171–199.